Role of carbon treating in piperazine oxidation

Yuying Wu[a], Gary T. Rochelle[a,*]

[a]*Texas Carbon Management Program, McKetta Department of Chemical Engineering, The University of Texas at Austin, 10500 Exploration Way, Austin, TX 78758, United States*

Abstract

Bench-scale experiments were performed to test the effects of carbon treating (8*30 mesh, lignite-based granular activated carbon from Nowata Filtration) on the oxidation of aqueous piperazine (PZ) at conditions of CO_2 capture. The combined mitigation with carbon treating and N_2 sparging was also tested. When carbon treating is applied, the UV-Vis absorbance at 320 nm, the NH_3 production rate, and the accumulation rate of dissolved Fe concentration and total formate concentration decrease. The effects of carbon treating last even when the carbon is bypassed, which is possibly due to the removal of catalytic degradation products. Therefore, it is better to apply carbon treating in the early stages of oxidation. Combining carbon treating and nitrogen sparging is more effective in oxidation mitigation than applying the methods separately. The amount of Fe removed by the carbon bed is greater than the result calculated from the solvent inventory and concentration difference of Fe in solvent, indicating that Fe colloids or other "soluble" Fe will dissolve into the solvent and replace the dissolved Fe that is adsorbed and removed. The carbon removes the degradation products that can complex with Fe^{3+}, even if they are not complexed. Since the source of Fe includes fly ash and corrosion, removing the complexing agents instead of all the available Fe is a more feasible target.

Keywords: CO_2; piperazine; oxidation; carbon treating; Fe

1. Introduction

5 m piperazine (PZ) is a promising second-generation solvent for amine scrubbing in post-combustion carbon capture due to its good thermal stability, high capacity, and high rate of CO_2 absorption.[1] During long-term operation, PZ can degrade into NH_3, oxopiperazine (OPZ), ethylenediamine (EDA), and heat stable salts including formate,[2] causing both economical losses and environmental concerns. Economically, degradation can cause amine loss, foaming and corrosion.[3] It also increases solvent viscosity and reduces the heat transfer performance in heat exchangers.[2] Volatile products such as NH_3 and volatile amine can raise environmental concerns.[3] Degradation products may catalyze the oxidation of solvent, causing the degradation rate to increase over time.[5] Dissolved Fe is limited by solubility, which increases as the solvent becomes more degraded.[2] Oxidation of PZ is expected to be

more significant than thermal degradation.[6] The identified products are listed in Fig. 1 in the order of production.

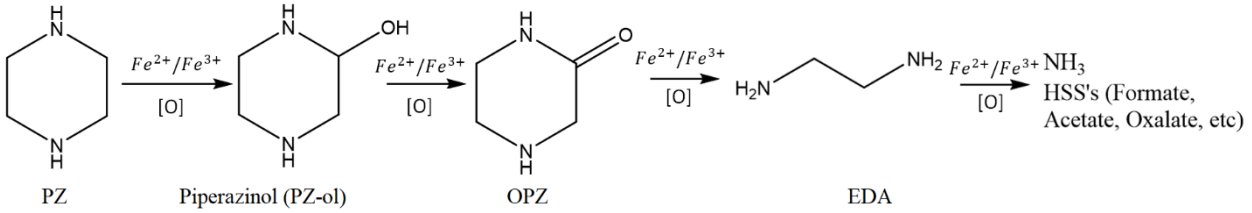

Fig. 1. Identified Oxidation products of PZ in probable order of production[2]

While granular activated carbon has been widely used in industry to remove contaminants, capture mercury compounds, and reduce foaming, the use of activated carbon is not common in amine scrubbing processes for CO_2 capture. A very limited period of carbon testing was performed at Technology Centre Mongstad (TCM) to address degradation of monoethanolamine MEA, but no firm conclusions were developed.[6] A 600-day continuous test of activated carbon was performed at a capture plant in Niederaussem using aqueous aminomethylpropanol (AMP) blended with PZ. The carbon removed coloring contaminants and dissolved Fe and Ni from the solvent, and stopped the increase in chloride concentration, but no significant reduction in total acid number was observed.[7] In a pilot plant test performed at the National Carbon Capture Center (NCCC), carbon treating showed potential to mitigate oxidation by reducing the NH_3 production. Activated carbon adsorbed Fe and Cr from the solvent, but the dissolved Fe did not decrease due to replenishment with the available soluble Fe.[8]

This work examines the species being removed with Fe. Two bench-scale experiments were performed to understand better the role of carbon treating. These experiments started with the end solvent collected from the NCCC 2019 campaign,[8] which contained 30 mmol/kg total formate, 0.13 mmol/kg Fe, 9.6 mmol/kg EDA, and 13.9 mmol/kg OPZ. 1.6 mmol/kg Li^+ in the solvent was used as a tracer to correct concentrations for changes in the water balance.

2. Experimental Apparatus

2.1. High Temperature Oxidation Reactor (HTOR)

Bench-scale experiments were performed in the high temperature oxidation reactor (HTOR), which cycles amine between a low-temperature reactor and a high-temperature oil bath up to 150 °C. This apparatus simulates solvent oxidation in the amine scrubbing process, with the reactor simulating the absorber, and the oil bath simulating the

stripper. The total inventory is 1.6 L, and the solvent has a flow rate of 0.2 L/min, set by the diaphragm pump. The peristaltic pump is set at the same flow rate to maintain the liquid height in the carbon bed and the bubble removal vessel. The inventory at low temperature is 1.0 L, and the inventory at hot rich condition is 0.6 L. The gas rate is 7.5 L/min, prepared by mixing compressed air with CO_2. The concentration of the CO_2 is set to provide 0.3 mol CO_2/mol PZ to avoid flashing at high temperature. Nitrogen sparging at 1 L/min and 10 cm effective height can be applied in the bubble removal vessel to remove dissolved oxygen. Previous HTOR tests were performed to understand the effects of N_2 sparging, catalysts, and inhibitors.[2] A glass column that is 15 mm in inner diameter and 300 mm tall was added between the peristaltic pump and the bubble removal vessel to serve as a carbon bed. 15.5 g of 8*30 mesh, lignite-based granular activated carbon was used in both the experiments presented in this work. This activated carbon is identical to that used in pilot plant testing at the National Carbon Capture Center in 2019.[8] The HTOR configuration is shown in Fig. 2. To ensure independent results between each run, the oxidative reactor, carbon bed, and bubble removal vessel were detached for cleaning with DDI water (distilled de-ionized water) and with 20 mM EDTA in DDI water.

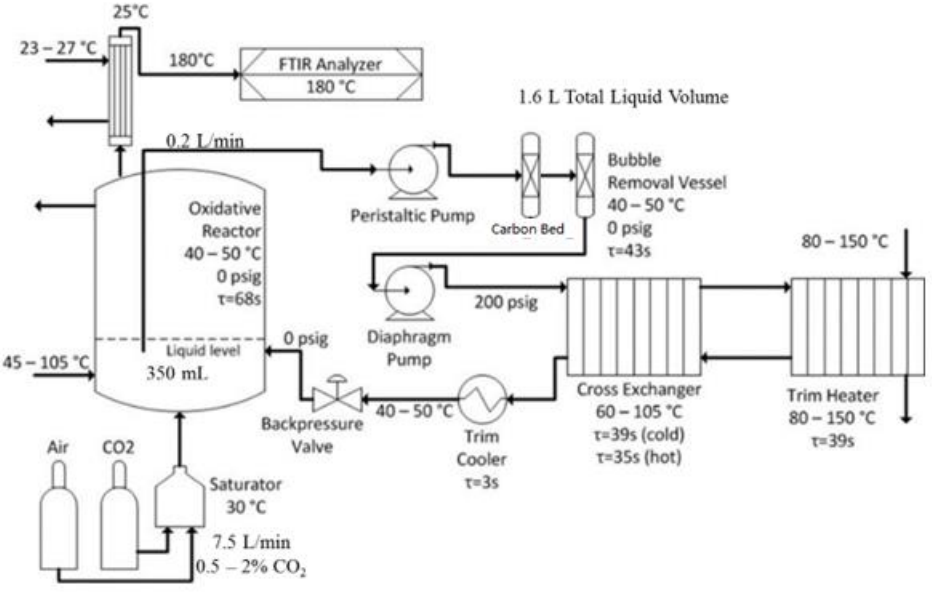

Fig. 2. High Temperature Oxidation Reactor (HTOR)

2.2. Carbon Adsorption Column (CAC)

A 25-mL burette was used as a carbon adsorption column (CAC). As shown in Fig. 3, the CAC was filled with 8*30 mesh, lignite-based granular activated carbon and plugged at the bottom with glass wool. The solvent flowing out from the column was fed through a peristaltic pump, which transferred the solvent back to the top of the column at 0.5 mL/s. The mass of the carbon in the column and the total solvent amount were measured to determine the carbon-to-solvent ratio, and the solvent was collected from the top for further analysis.[9]

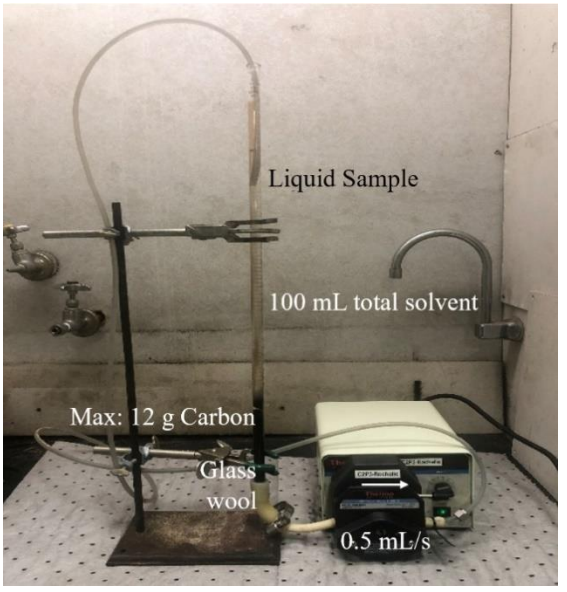

Fig. 3. Carbon adsorption column

3. Analytical Methods

3.1. Anion IC (Ion Chromatography)

The concentrations of heat stable salts including formate, acetate, glycolate, and oxalate generated from PZ degradation were measured with anion chromatography. A Dionex ICS-6000 Ion Chromatography System was used with an IonPac AG15 guard column and an IonPac AS15 analytical column.[8,9] The eluent was 2 to 40 mM potassium hydroxide in analytical grade DDI water. A conductivity detector was used to analyze for the conductivity output. Standards between 0.01 mmol/kg and 0.5 mmol/kg in DDI water were used to obtain the elution time of the species and a calibration curve. The samples contained a large sulfate peak and a small oxalate peak. The oxalate peak was on the tail of the sulfate peak and was estimated by treating the tail as the baseline. The total heat stable salts, which

included both the free anions and the anions combined with the amines as amides, were analyzed after breaking the bond between the salts and the amine by treating with 10 N NaOH 1:1 volumetrically for 24 hours. The treated samples were diluted 50 times with DDI water in a 1.5 mL plastic vial, and 25 µL was used for each injection. The total acids is equal to the sum of total formate, total acetate, and 2 times total oxalate. The same scripts are used to analyze for heat stable salts and total heat stable salts. Table 1 includes the species in most degraded samples and their elution time. The detailed script is included in Table A-1 in Appendix A.

Table 1. Species quantified by Anion IC

Species	Elution Time (minutes)
Acetate	19.9
Formate	20.7
Sulfate	29.9
Oxalate	30.0
Nitrate	32.7

3.2. Cation IC

PZ and other cation degradation products were measured with cation chromatography. A Dionex™ ICS-6000 Capillary HPIC™ system was used with an IonPac CG 17 guard column and an IonPac CS 17 analytical column.[10] The eluent was 5.5 to 33 mM of methanesulfonic acid in analytical grade DI water. A conductivity detector was used to analyze for the conductivity output. Standards between 0.01 mmol/kg and 0.5 mmol/kg in DDI water were used to obtain the elution time of the species and a calibration curve. The samples were diluted 10000 times gravimetrically with DDI water in a 1.5 mL plastic vial, and 25 µL was used for each injection. Table 2 gives the species in most degraded samples and their elution time. The detailed script is included in Table A-2 in Appendix A.

Table 2. Species quantified by Cation IC

Species	Full Name	CAS #	Time (minutes)
NH_4^+			5.0
OPZ	2-oxopiperazine	5625-67-2	6.8
FPZ	1-formylpiperazine	7752-92-2	7.4
EDA	Ethylenediamine	107-15-3	17.9
PZ	Piperazine	110-85-0	20.2
HEP	1-(2-hydroxyethyl)piperazine	103-76-4	21.7
MPZ	1-methylpiperazine	109-01-3	22.4
EPZ	1-ethylpiperazine	5308-25-8	23.7

DMPZ	1,4-dimethylpiperazine	106-58-1	25.2
AEP	Aminoethylpiperazine	140-31-8	29.3

3.3. ICP-OES

A Varian 10-ES Axial ICP-OES was used to analyze metals by the specific wavelength of UV light emitted in argon plasma flame at 7000 K.[2] 0.32 mL samples were diluted with a dilution factor of 25X by 7.68 mL with 2 wt % nitric acid to allow for multiple analyses, and standards between 0.5 ppm and 25 ppm were prepared for each run. For samples with low metal concentrations, a smaller dilution factor was used to ensure the intensity of metals peaks are larger than 10^6, significantly higher than the typical 100 noise signals. Since PZ can interfere with the absorbance of light in the measurement, the standards were prepared with the same concentration of PZ added to eliminate interference. For each element, two to three high intensity wavelengths that are not interfered with by other metals were used, and three measurements were performed at each wavelength. The average of the measurements is reported, and the standard deviation is usually within 2% to 3%. Since ICP-OES excites all metals to the highest state and analyzes the electromagnetic radiation, it cannot distinguish between different ions or oxidation states of the same element, and the results represent the total amount of specific metals in the samples. The characteristic wavelengths of the commonly analyzed metals are listed in Table 3.

Table 3. Characteristic wavelengths for ICP-OES metal quantification

Elements	*Measure Wavelengths (nm)*		
Lithium (Li)	670.783	610.365	
Potassium (K)	766.491	769.897	
Iron (Fe)	234.350	238.204	259.940
Chromium (Cr)	205.560	206.158	267.716
Nickel (Ni)	216.555	221.648	231.604
Manganese (Mn)	257.610	259.372	260.568
Copper (Cu)	213.598	224.700	324.754

3.4. UV-Vis

The UV-Vis measurements were performed with two instruments: a NanoDrop™ One Microvolume UV-Vis spectrophotometer, and a Varian Cary 5000 UV-Vis-NIR spectrophotometer. The NanoDrop worked well with samples that have high absorbance, while the Varian Cary can only measure in a range between 0 and 2.5 A. 1.5 µL of sample was analyzed with the NanoDrop first to estimate absorbance range. The sample was then diluted to close to 1 A with water for a second measurement with the Varian Cary. 3.5 mL of the diluted sample was injected in a disposable cuvette with a light path of 10 nm. A dilution-corrected absorbance was reported by multiplying the measured absorbance and the dilution factor. The instrument was calibrated with zero transmittance and a water blank before each analysis.[9]

4. Experiment Results

4.1. Identification of the UV-Vis Absorbance Peak at 320 nm

Different metal ions were added to clean and degraded samples. While the addition of $(NH_4)_2Fe(SO_4)_2$ did not produce any peak at 320 nm or 538 nm, the addition of $NH_4Fe(SO_4)_2{\cdot}12H_2O$ replicated the peak at 320 nm, shown as the purple curve in Figure 4. $NH_4Fe(SO_4)_2{\cdot}12H_2O$ in 5 m PZ absorbs at 293 nm instead of 320 nm, indicating that the 320 nm peak was caused by Fe^{3+} complexed with one or several degradation products of PZ. Fe^{3+} was also added to clean PZ spiked with major degradation products, including NH^{4+}, EDA, formate, acetate, and oxalate, but the absorbance peak remained at 293, indicating these species alone were not complexing with Fe^{3+} to absorb at 320 nm.

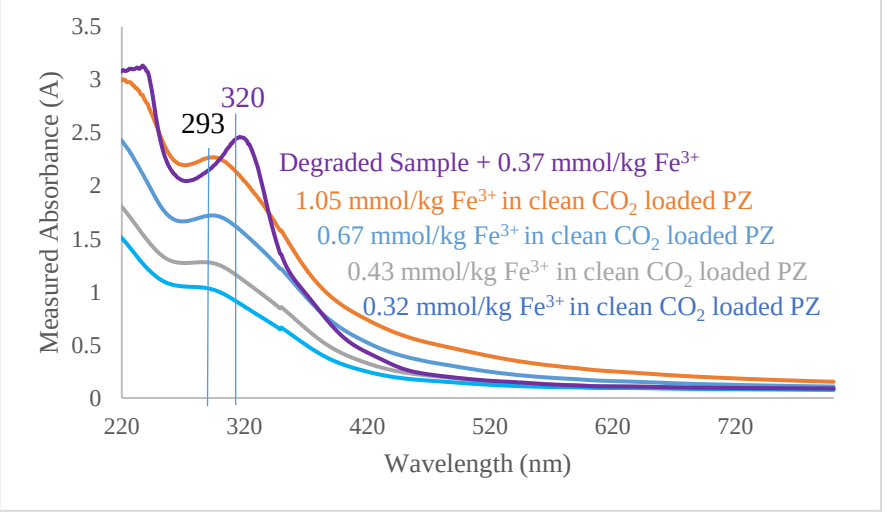

Fig. 4. Absorbance of Fe^{3+} in clean PZ and degraded sample

There is a linear relationship between the increase in absorbance and the added Fe^{3+} shown in Fig. 5, indicating that there is excess degradation product ready to complex with the Fe^{3+}. Fe^{3+} is not the only species contributing to the 320 nm peak as the Fe^{3+} concentration calculated by UV-Vis was much higher than the Fe concentration given by ICP. As shown in Fig. 6, Ni^{2+}, Cr^{3+}, and Mn^{2+} also absorb close to 320 nm, and can add to the peak intensity at 320 nm. It is probable that the 320 nm peak represents some overall metal level in the solvent.[9] The metal concentrations shown in this work were all measured by ICP.

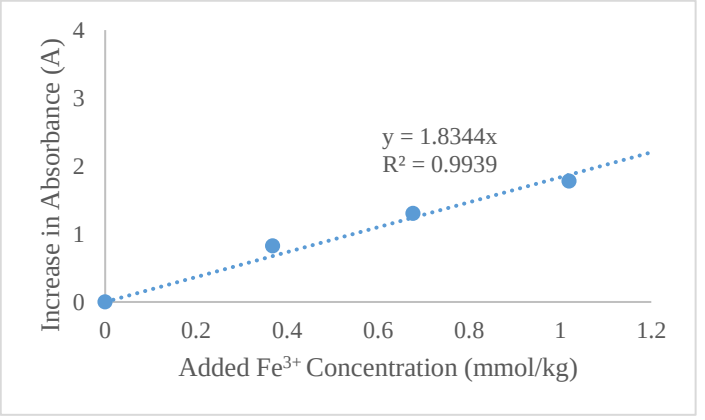

.

Fig. 5. Calibration curve of Fe^{3+}complex at 320 nm

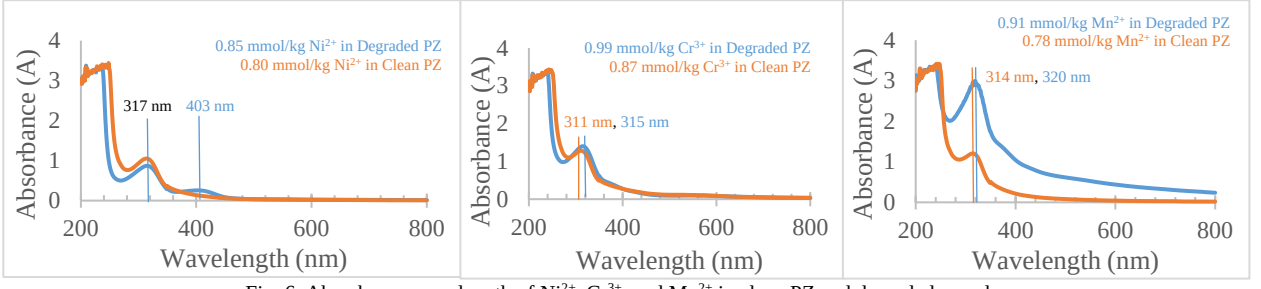

Fig. 6. Absorbance wavelength of Ni^{2+}, Cr^{3+}, and Mn^{2+} in clean PZ and degraded samples

4.2. HTOR Experiments on Moderately Degraded PZ with Carbon Treating and Nitrogen Sparging

Two parallel experiments were performed to test the effect of carbon treating on the oxidation of the NCCC 2019 end solvent in the HTOR. In both experiments, nitrogen sparging was applied in the middle of the experiment, testing the combined mitigation effect of carbon treating and nitrogen sparging. A 7.5 L/min synthetic flue gas was created by mixing air with 0.5% CO_2 to maintain a loading of 0.25 mol CO_2/mol PZ, which is close to the lean loading in real

plant operations. The solvent was cycled between 55 °C and 150 °C at 0.2 L/min. To exclude the effect of water introduction or removal on concentration, the concentration of all species was corrected with a normalization factor equal to Li in sample divided by initial Li concentration measured by ICP. The process changes in HTOR 28 and HTOR 29 are recorded in Table 4 and Table 5. In HTOR 28, foaming was observed at the baseline condition and disappeared within 24 hrs after carbon treating was applied. The system experienced in HTOR 28 a severe water balance issue in the first 140 hrs, so only the data after 140 hrs are reported. Starting from 482 hrs, increased accumulation rates were observed on the indicators of oxidation, including Fe concentration, UV-absorbance, NH_3 production rate and total formate concentration. Therefore, it was believed that the activated carbon was depleted, and only N_2 sparging was taking effect between 482 hrs and the end of the experiment.

Table 4. Process changes during HTOR 28

Time (hrs)	Process Change	Length of Test (hrs)
140	Baseline (No carbon or N_2)	74
214	15.5 g Carbon treating	170
384	N_2 sparging (10 cm liquid depth) + carbon treating	98
482	N_2 sparging (10 cm liquid depth) + depleted carbon	96
578	End of experiment	

Table 5. Process changes during HTOR 29

Time (hrs)	Process Change	Length of Test (hrs)
0	15.5 g carbon treating	142
142	Baseline (No carbon or N_2 sparging)	272
414	N_2 sparging (10 cm liquid depth)	186
600	N_2 sparging (20 cm liquid depth)	64
664	End of experiment	

4.2.1. PZ Concentration

The PZ concentration normalized by Li is plotted in Fig. 7 (HTOR 28) and Fig. 8 (HTOR 29). Since the concentration of PZ is high, the loss rate is not accurate enough in regions with only 4 or 5 data points, but it is clear that qualitatively both carbon treating and N_2 sparging reduced the PZ loss rate, and the combined treating mitigated

oxidation more significantly. Models consisting of four connecting linear regression curves that minimize the sum of squared error for the whole data set were created, and the slopes are shown in the respective figures.

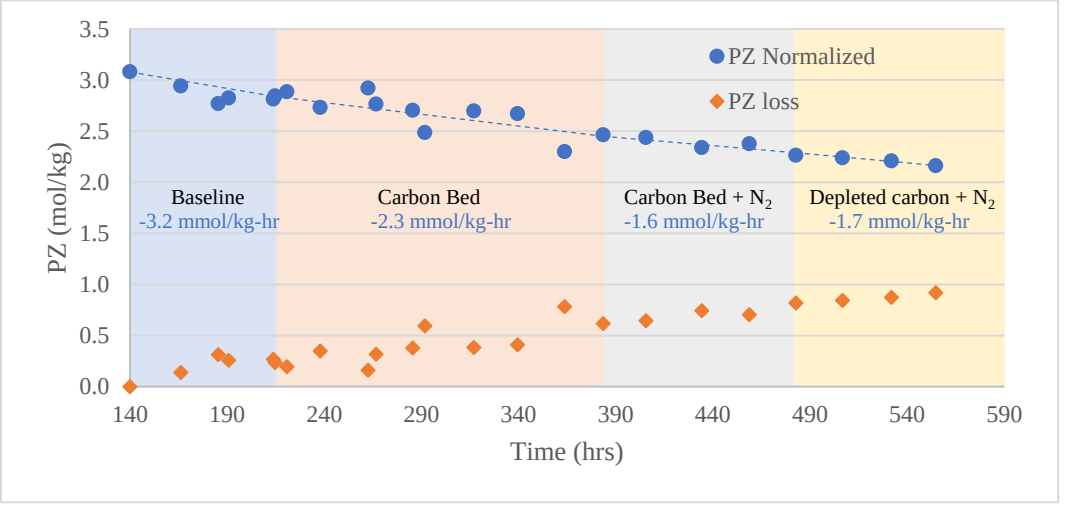

Fig. 7. Normalized PZ in HTOR 28 (0.5% CO_2, 55 °C to 150 °C, NCCC 2019 end solvent, carbon bed, and N_2 sparging)

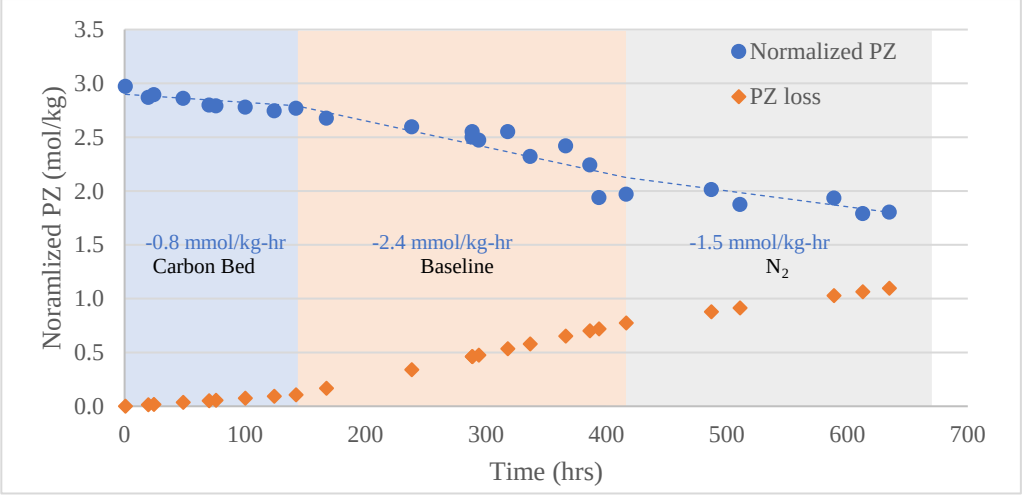

Fig. 8. PZ normalized by Li in HTOR 29 (0.5 % CO_2, 55 °C to 150 °C, NCCC 2019 end solvent, carbon bed, and N_2 sparging)

4.2.2. NH_3, Fe, and Absorbance

While NH_3 is not a direct oxidation product of PZ as shown in Fig. 1, it is an indicator of the net oxidation rate. A strong correlation between NH_3 production rate, Fe concentration, and the dilution-corrected absorbance was observed, and is plotted with cumulative NH_3 production in Fig. 9 (HTOR 28) and Fig. 10 (HTOR 29).

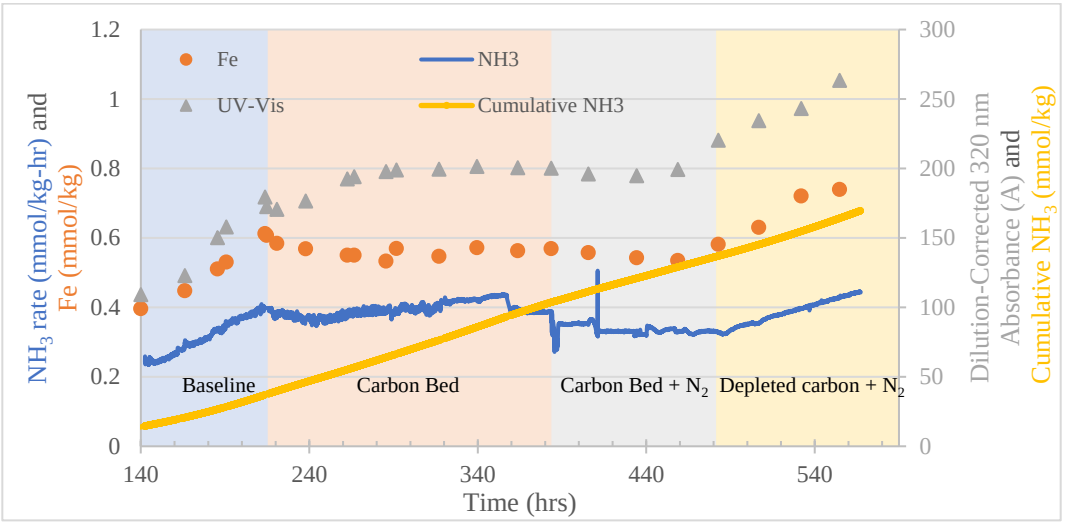

Fig. 9. Correlation of cumulative NH_3 production, NH_3 production rate, Fe concentration, and dilution-corrected absorbance at 320 nm in HTOR 28 (0.5% CO_2, 55 °C to 150 °C, NCCC 2019 end solvent, carbon bed, and N_2 sparging)

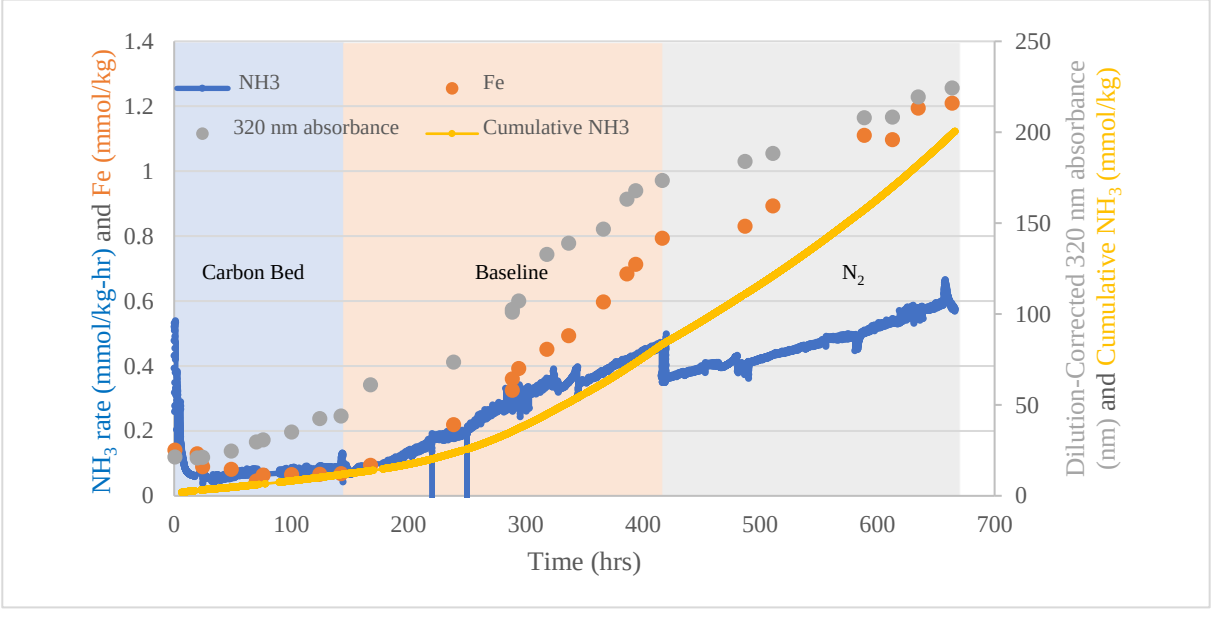

Fig 10. Correlation of cumulative NH_3 production, NH_3 production rate, Fe concentration, and dilution-corrected absorbance at 320 nm in HTOR 29 (0.5% CO_2, 55 °C to 150 °C, NCCC 2019 end solvent, carbon bed, and N_2 sparging)

4.2.3. OPZ, EDA, and Total N Products

The OPZ, EDA, and total N products are plotted in Fig. 11 (HTOR 28) and Fig. 12 (HTOR 29). The total N products represents the total amount of N in the degradation products are cumulative NH_3 production, OPZ concentration, EDA

concentration, MPZ concentration, AEP concentration, and FPZ concentration.

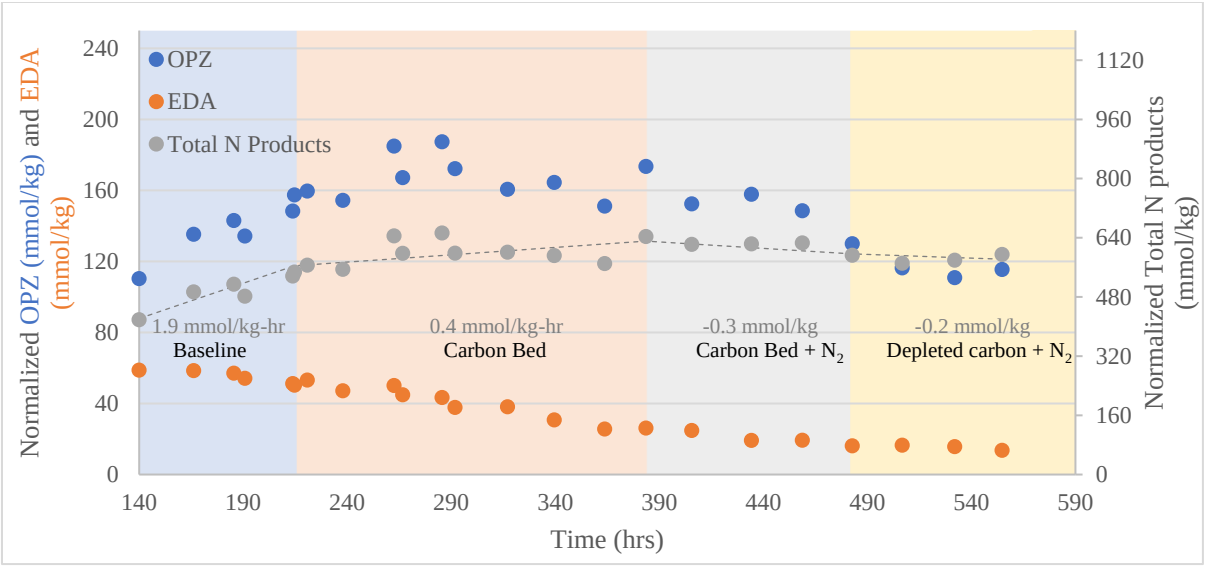

Fig. 11. Normalized OPZ concentration, EDA concentration, and total nitrogen products in HTOR 28 (0.5% CO_2, 55 °C to 150 °C, NCCC 2019 end solvent, carbon bed, and N_2 sparging)

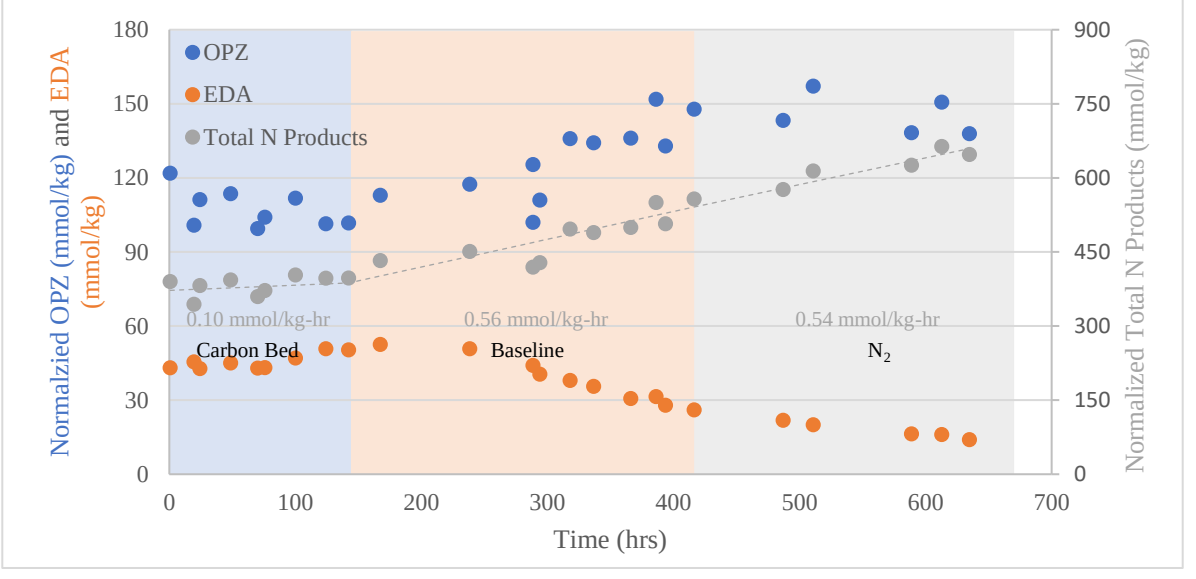

Fig. 12. Normalized OPZ concentration, EDA concentration, and total N products in HTOR 29 (0.5 % CO_2, 55 °C to 150 °C, NCCC 2019 end solvent, carbon bed, and N_2 sparging)

4.2.4. Total Formate, Total Acids, and Total Oxidized Carbon

The concentrations of total formate concentration, total acids, and total oxidized carbons are plotted in Fig. 13

(HTOR 28) and Fig. 14 (HTOR 29). The total acids is equal to the sum of total formate concentration, total acetate concentration, and 2 times total oxalate concentration, and the total oxidized carbon is the sum of oxidized carbon in degradation products, which is equivalent to the sum of the total acids and OPZ.

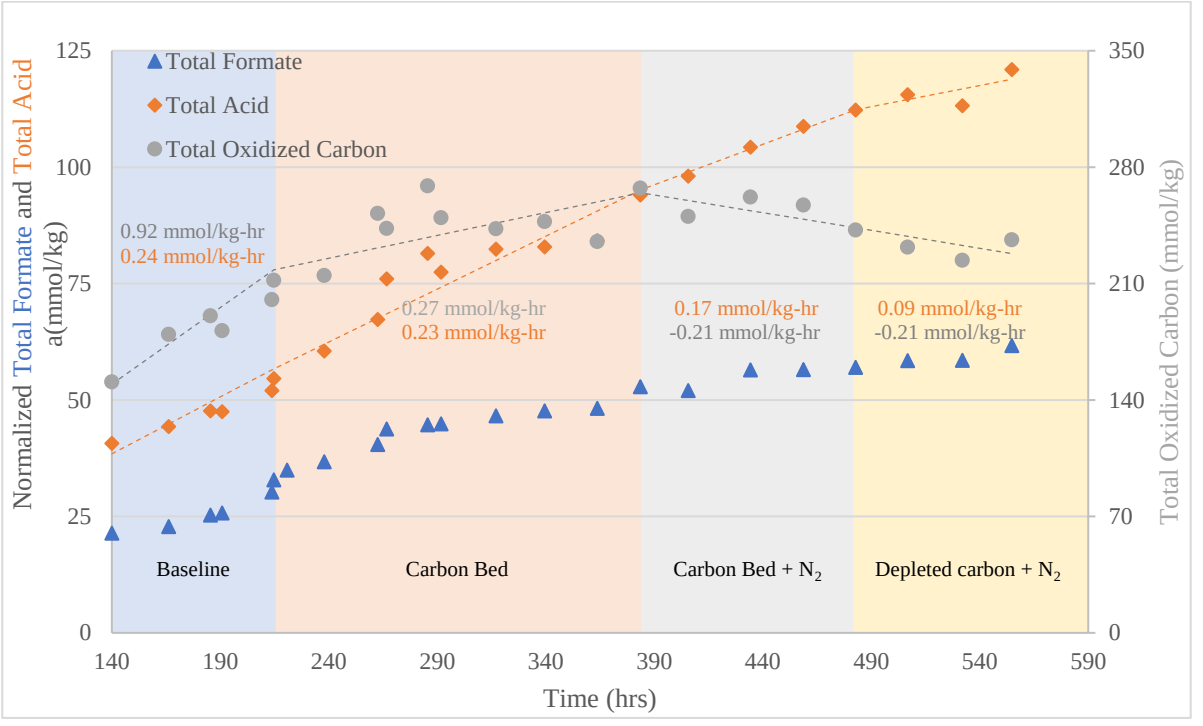

Fig. 13. Normalized total formate concentration, total acids, and total oxidized carbon in HTOR 28 (0.5% CO_2, 55 °C to 150 °C, NCCC 2019 end solvent, carbon bed, and N_2 sparging)

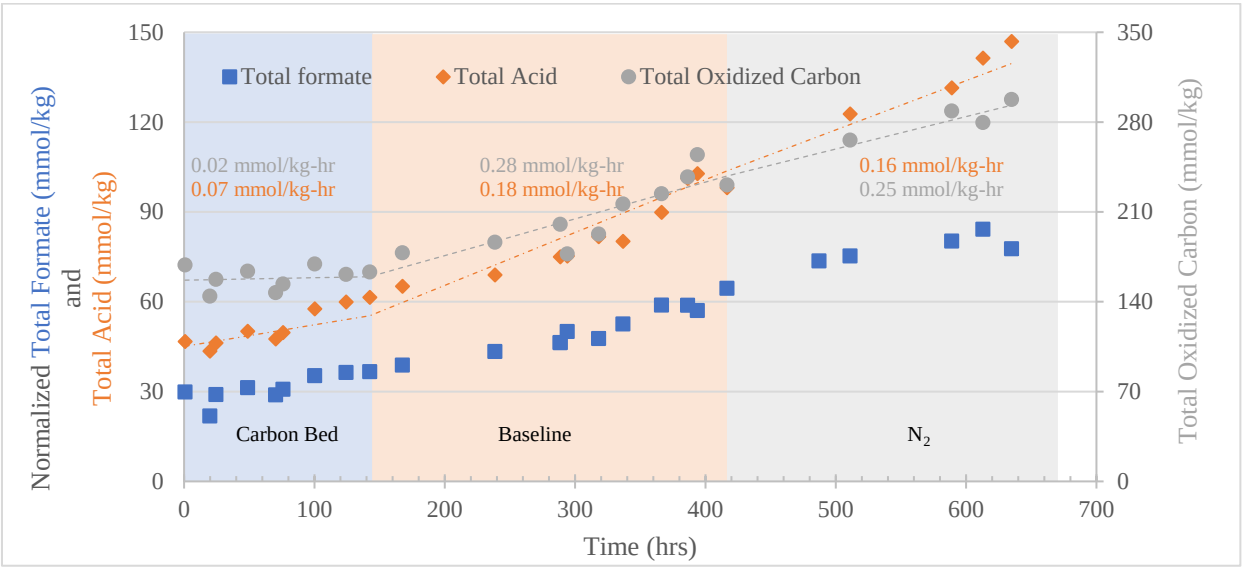

Fig. 14. Normalized total formate concentration, total acids, and total oxidized carbon in HTOR 29 (0.5 % CO_2, 55 °C to 150 °C, NCCC 2019 end solvent, carbon bed, and N_2 sparging)

4.2.5. Cr, Mn, and Ni

The normalized stainless steel metal ion concentrations are shown in Fig. 15 and Fig. 16. All the metal ion concentrations increased when there was no carbon bed applied, due to corrosion of stainless steel. The increase of Ni concentration was not a function of carbon treating or nitrogen sparging. The Cr concentration and Mn concentration decreased when there was a working carbon bed, which matched the previous observation that the carbon bed can remove dissolved Mn at a low rate.

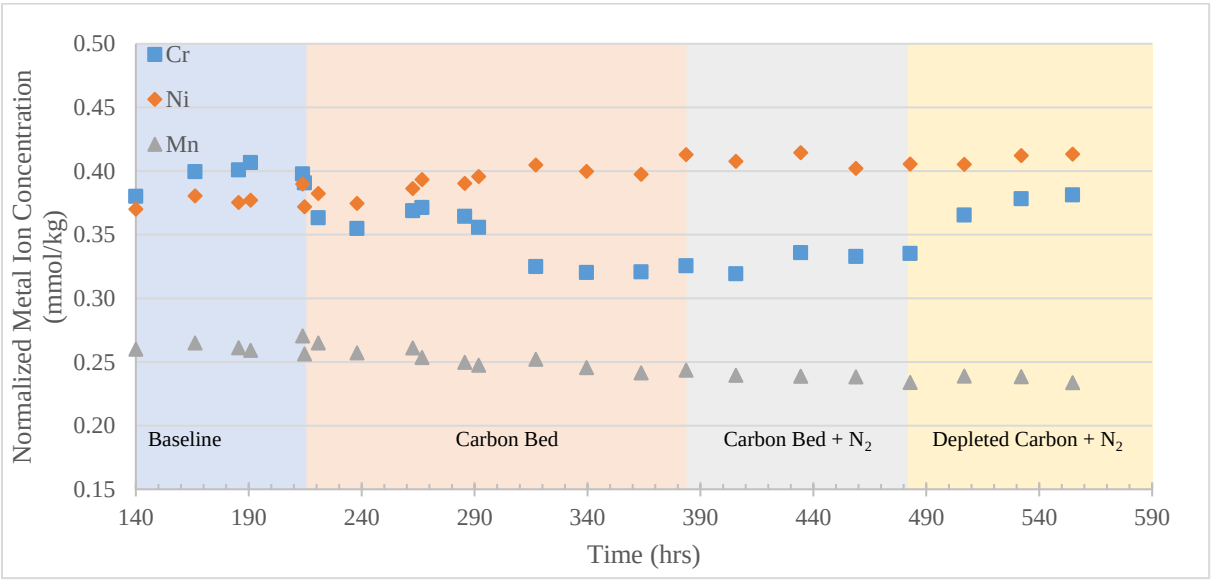

Fig. 15. Normalized metal ion concentrations in HTOR 28 (0.5 % CO_2, 55 °C to 150 °C, NCCC 2019 end solvent, carbon bed, and nitrogen sparging)

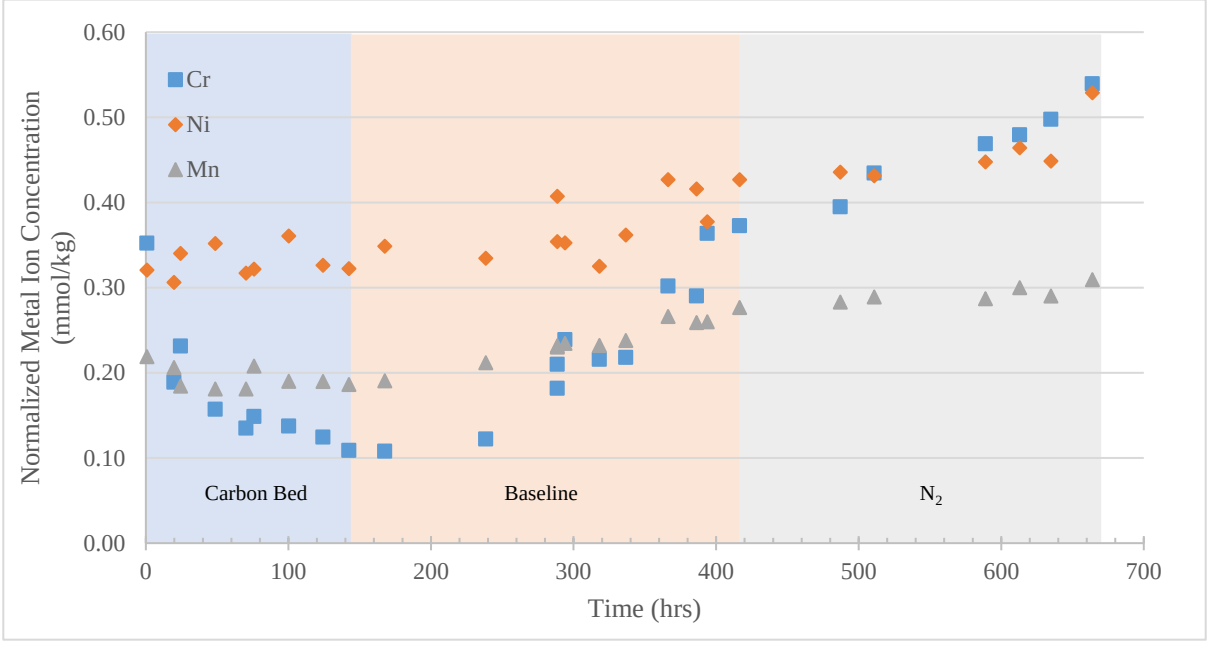

Fig. 16. Normalized metal ion concentrations in HTOR 29 (0.5 % CO_2, 55 °C to 150 °C, NCCC 2019 end solvent, carbon bed, and nitrogen sparging)

4.2.6. Quantification of Adsorbed Fe

The Fe removed by the carbon bed was quantified by treating the carbon with 0.2 N H_2SO_4 and measuring the Fe

concentration in the eluent. The integrated Fe concentration on the carbon per rinse is shown in Table 6 and Fig. 17. In each experiment, 8 batches of H_2SO_4 were added, and each batch was drained completely before the new batch was added. The Fe concentration in the final rinse is under the detection limit (0.006 mmol/kg) in ICP-OES analysis for complete Fe removal.

Table 6. Integrated Fe on the initial carbon, HTOR 28 end carbon, and HTOR 29 end carbon

	Integrated Fe (mmol/kg carbon)		
	Initial carbon	HTOR 28 end carbon	HTOR 29 end carbon
1	25.32	36.86	22.82
2	33.25	52.63	31.95
3	34.57	57.80	38.59
4	35.07	61.36	43.22
5	35.49	62.98	46.61
6	35.91	64.03	47.51
7	36.34	65.70	47.99
8		67.37	48.44
Total Fe Removed		0.30 (mmol/kg Solvent)	0.12 (mmol/kg Solvent)

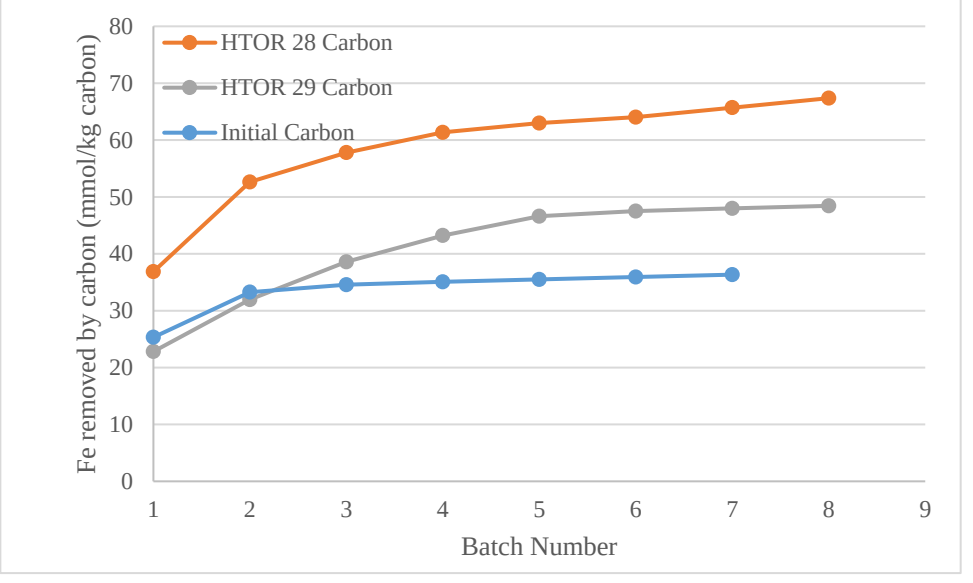

Fig. 17. Integrated Fe concentration on carbon (mmol/kg carbon) on HTOR 28 end carbon, HTOR 29 end carbon, and initial carbon

The decrease of Fe concentration in solvent in both experiments was compared to the Fe removed by the carbon bed as shown in Fig. 18. The Fe removed by carbon (0.30 mmol/kg in HTOR 28, 0.12 mmol/kg in HTOR 29) was significantly higher than the difference of Fe concentration (0.07 mmol/kg) before and after carbon treating. Similar to results from the NCCC 2019 pilot test,[8] this concentration difference is much higher than the difference of Fe before and after carbon treating, confirming that soluble solid Fe^{2+}/Fe^{3+} dissolved to continuously replenish the Fe in solution.

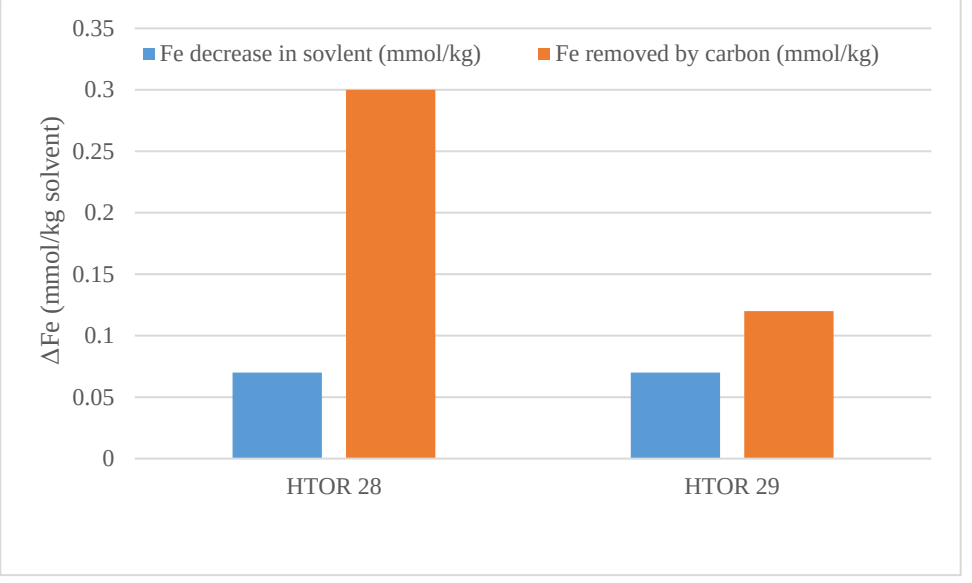

Fig. 18. Comparison of the Fe concentration decrease in solvent and Fe removed by carbon bed

4.3. Removal of the Complexing Agents by Activated Carbon

Additional experiments were performed to determine if the complexing agent was removed by the activated carbon. Figs 19 and 20 show the UV-Vis absorbance when different amounts of Fe^{3+} were added to a degraded solvent and carbon-treated degraded solvent. $NH_4Fe(SO_4)_2 \cdot 12H_2O$ was dissolved in water and added to samples as a source of Fe^{3+}. The solvent in Fig. 19 was collected after 2100 hrs of operation in the NCCC 2018 campaign[12], and the solvent in Fig. 20 was the same solvent after 450 hrs of carbon treatment in the CAC.

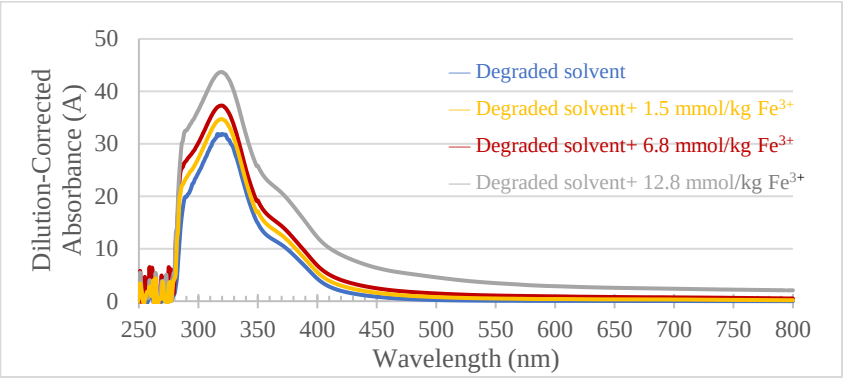

Fig. 19. UV-Vis absorbance profile of NCCC #3706 with variable Fe^{3+} addition

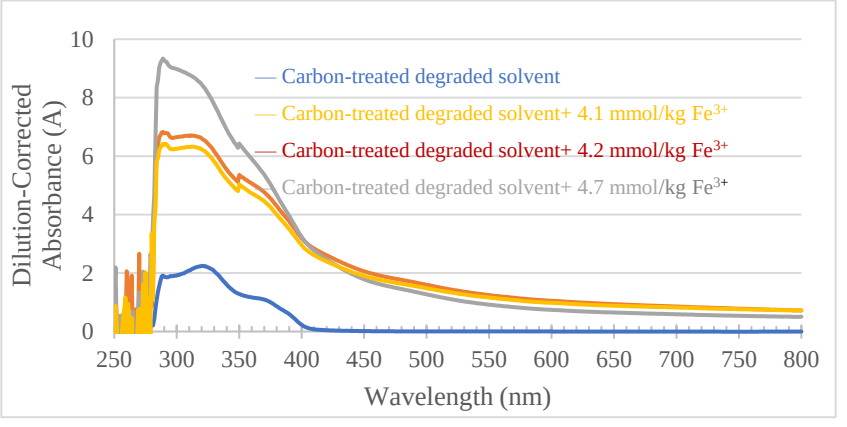

Fig. 20. UV-Vis absorbance profile of carbon-treated degraded solvent with variable Fe^{3+} addition

5. Discussion

5.1. Accumulation Rates of Important Degradation and Corrosion Products

No NH^{4+} peak above limit of detection was observed in both experiments, suggesting a low $NH4^{+}$ concentration in solvent. Table 6 and Table 7 show a summary of the species accumulation rates measured in HTOR 28 and HTOR 29. A least-square fit regression line is used in each region to calculate the rate of accumulation for each species.

Table 6. Summary of degradation and corrosion products, and PZ oxidation rate in HTOR 28 (+/- indicates standard deviation)

Species	Baseline	Carbon Bed	Carbon Bed + N_2 Sparging	Depleted Carbon + N_2 Sparging
Gas-phase NH_3 rate ($\mu mol/kg\text{-}hr^2$)	2.42 ± 0.01	0.27 ± 0.01	-0.23 ± 0.01	1.40 ± 0.00

PZ (mmol/kg-hr)	-4.0 ± 1.3	-2.8 ± 0.6	-1.4 ± 0.5	-2.0 ± 0.2
320 nm absorbance (A/hr)	1.00 ± 0.10	0.17 ± 0.09	0.01 ± 0.05	0.69 ± 0.11
Total formate (mmol/kg-hr)	0.14 ± 0.3	0.08 ± 0.01	0.05 ± 0.02	0.06 ± 0.4
Fe (μmol/kg-hr)	2.9 ± 0.2	0.0 ± 0.0	-0.5 ± 0.3	2.4 ± 0.8
OPZ (mmol/kg-hr)	0.52 ± 0.12	0.01 ± 0.07	-0.29 ± 0.10	-0.02 ± 0.12
Cr (μmol/kg-hr)	0.26 ± 0.15	-0.37 ± 0.07	0.14 ± 0.07	0.33 ± 0.11
Ni (μmol/kg-hr)	0.21 ± 0.09	0.20 ± 0.03	-0.08 ± 0.06	0.17 ± 0.06
Mn (μmol/kg-hr)	0.09 ± 0.08	-0.11 ± 0.02	-0.08 ± 0.02	-0.11 ± 0.05

Table 7. Summary of degradation and corrosion products, and PZ oxidation rate in HTOR 29 (+/- indicates standard deviation)

Species	Carbon Bed	Baseline	N_2 Sparging
Gas-phase NH_3 rate ($\mu mol/kg\text{-}hr^2$)	0.30 ± 0.01	1.51 ± 0.01	0.81 ± 0.02
PZ (mmol/kg-hr)	-1.4 ± 0.2	-2.6 ± 0.4	-1.5 ± 0.5
320 nm absorbance (A/hr)	0.18 ± 0.01	0.52 ± 0.03	0.23 ± 0.02
Total formate (mmol/kg-hr)	0.07 ± 0.02	0.12 ± 0.01	0.05 ± 0.04
FPZ (mmol/kg-hr)	0.06 ± 0.01	0.11 ± 0.01	0.05 ± 0.02
Total oxalate (mmol/kg-hr)	0.008 ± 0.005	0.045 ± 0.004	0.026 ± 0.004
Fe (μmol/kg-hr)	-1.4 ± 0.2	2.7 ± 0.2	2.3 ± 0.4
OPZ (mmol/kg-hr)	-0.08 ± 0.05	0.16 ± 0.04	-0.03 ± 0.04
Cr (μmol/kg-hr)	0.16 ± 0.14	1.25 ± 0.24	0.63 ± 0.12
Ni (μmol/kg-hr)	0.08 ± 0.06	0.43 ± 0.27	0.50 ± 0.25
Mn (μmol/kg-hr)	0.12 ± 0.05	0.35 ± 0.05	0.11 ± 0.07

5.2. Absorbance

In both experiments, the UV absorbance at 320 nm increased at a slower rate when the carbon bed was applied, probably because the carbon bed was removing the UV-absorbing species. N_2 sparging reduces the UV accumulation

rate by 0.3 A/hr, and this rate is not related to the initial rate of accumulation before N_2 sparging. No change on N_2 sparging was observed with greater liquid depth. The combined treatment of carbon bed and N_2 sparging resulted in a lower rate compared to carbon treating or N_2 sparging alone

In HTOR 29, the baseline rate is 0.52 A/hr, much slower than the 1 A/hr in the baseline condition in HTOR 28. Although the carbon bed was bypassed, the removal slows down the accumulation of UV-absorbing components, indicating that applying carbon treating in the early stages of oxidation can be more effective.

5.3. Fe, Cr, and Mn

Compared to the initial Fe concentration of 0.13 mmol/kg, the Fe concentration throughout the HTOR experiments was considerably higher, indicating that the Fe solubility limit at the HTOR operating condition is higher than the solubility limit at NCCC operating conditions. Carbon treating resulted in a lower Fe accumulation rate as the activated carbon adsorbed the Fe, and N_2 sparging can reduce the Fe accumulation rate due to the reduced degradation rate.[2] The combination of carbon treating and N_2 sparging is more effective than applying one mitigation method. After treatment, Fe concentration continued to increase at the same rate once the carbon bed is bypassed. Therefore, to maintain low Fe concentration in operation, the carbon bed needs to be kept on constantly.

In both HTOR 28 and 29, the Mn decreased when there was a working carbon bed, which matched the previous observation that the carbon bed removes dissolved Mn at a low rate. The Cr concentration decreased when the carbon bed was turned on but reached steady state at 0.32 mmol/kg in HTOR 28 and 0.11 mmol/kg in HTOR 29.[9]

5.4. NH_3

The NH_3 production rate may represent the oxidation rate of the solvent and its degradation products. In both experiments, the increase in NH_3 production rate stopped when carbon treating was applied, but there was no step change in the NH_3 rate. After N_2 sparging was applied, there was a step decrease in the NH_3 production rate, after which the rate continued to decrease. In previous HTOR experiments with no carbon bed, the NH_3 production rate decreased when sparging was initially applied, but still increased as the experiment continued with N_2 sparging.[2] From 483 hrs to the end of the experiment, the results represented the mitigation effects of nitrogen sparging only. The slope of the NH_3 rate was 50% smaller with N_2 sparging than the baseline condition. The cumulative NH_3 produced throughout the HTOR 28 was 183.5 mmol/kg, or 0.34 mmol/kg-hr. The cumulative NH_3 production was

200.5 mmol/kg in HTOR 29, or 0.30 mmol/kg-hr. In HTOR 29, after the carbon bed is bypassed, the NH_3 rate increase in the base condition is lower than that in HTOR 28. This indicates that the effect of carbon bed lasted, possibly due to the removal of catalytic degradation products or NH_3 precursors.

To conclude, N_2 sparging reduces the NH_3 production rate and its rate of increase. Carbon treating does not reduce NH_3 production rate but reduces its rate of increase. Combining the two mitigation methods is more effective than applying either method individually.

5.5. PZ

In HTOR 28, the overall PZ loss rate was 2.1 ± 0.2 mmol/kg-hr, while in HTOR 29 it was 1.9 ± 0.1 mmol/kg-hr. The overall PZ loss rates were 6 times the NH_3 production rate, and since little PZ was observed in the gas outlet, only 1 mol of NH_3 was produced when 6 mols of PZ were oxidized, suggesting a different oxidation mechanism than observed in previous experiments, which produced 1 mol of NH_3 per mol of oxidized PZ.[2] It is also possible that the precursor of NH_3 was adsorbed by the carbon and removed from the solvent, thereby shifting the equilibrium and reducing the total NH_3 production.

The PZ loss rate at the baseline condition in HTOR 29 was lower than in HTOR 28, indicating that the effects of carbon treating in the first 140 hrs lasted after the carbon was bypassed due to the removal of possible catalytic products. Therefore, it is better to apply carbon treating in the early stages of oxidation.

5.6. OPZ and EDA

In both experiments, OPZ concentration increased at the baseline condition. By applying carbon treating or N_2 sparging, the OPZ concentration started decreasing, and the mitigation effect is better when the two methods are combined. The OPZ concentration increase at the baseline condition is lower in HTOR 29 than in HTOR 28, suggesting the benefits of applying carbon treating early.

In HTOR 29, EDA concentration increased first and then decreased, which was similar to previous observations in both bench-scale and pilot plants without any treatment.[9] In both experiments, EDA concentration decreased steadily after reaching a maximum, and no significant difference in decomposition rate was observed, so the degradation of EDA concentration is independent of the application of the carbon bed or N_2 sparging.

5.7. Total Formate

Mitigation effects on formate accumulation were observed for both carbon treating and N_2 sparging. Compared to HTOR 28, the formate accumulation rate at baseline conditions in HTOR 29 is lower, suggesting that carbon treating may remove precursors of formate. Therefore, the rate of formate accumulation was reduced even after the carbon was bypassed. So, applying carbon treating in the early stage of oxidation may be more effective.

5.8. Removal of complexing agents

When Fe^{3+} was added to a carbon-treated degraded solvent, the peak at 293 nm increased instead of the peak at 320 nm (figs. 19 and 20). This indicates that the complexing agents were all removed by the carbon, so that the Fe^{3+} was not complexed and the measured absorbance appeared at 293 nm instead of 320 nm. The apparent solubility limit of Fe^{3+} in the solvent decreased from 12.8 mmol/kg to 4.2 mmol/kg. Therefore, carbon treating may be useful in preventing Fe from further dissolving into the degraded solvent if no further complexing agent is produced in the solvent.

Both experiments showed that Fe can be removed by activated carbon, but more soluble Fe can redissolve if the complexing agents remain in the solvent. This explains why the dissolved Fe remained low after Fe additions in clean solvent at both bench and pilot scale and shows that adding sulfide to precipitate Fe had no effect on dissolved Fe concentration,[2] since the concentration of the complexing agents was minimal in clean solvent. Therefore, instead of removing all the Fe available, removing all the complexing agents from degradation will be a more viable method.

5.9. Comparison with pilot plant in Niederaussem

A pilot plant in Niederaussem tested the activated carbon in AMP/PZ solvent. It was observed that the solvent color became lighter. However, since no UV-Vis analysis results were reported, it was unclear if the absorbance at 320 nm decreased. The concentration of Fe and Ni decreased.[7] However, no effects were observed on the accumulation of degradation products,[7] unlike the HTOR experiments presented in this work. The difference is possibly due to the different type of activated carbon. In Niederaussem, the carbon used was a granular carbon with a particle diameter of 0.6-2,36 mm (Type L 8x30 C from Wocklum Chemie; steam-activated active carbon produced from coconuts by pyrolysis),[7] while the activated carbon used in the HTOR experiments was 8*30 mesh, lignite-

based granular activated carbon from Nowata Filtration. Based on the pilot plant and bench-scale work, the activated carbon from Nowata Filtration can mitigate the oxidation of piperazine solvent. More research on the types of activated carbon can be done to explore options more suitable for amine-based carbon capture process.

6. Conclusions

- Carbon treating is effective in removing degradation and corrosion products and mitigating oxidation in the HTOR. When carbon treating is applied, the increase in NH_3 rate slows down, the UV-Vis absorbance at 320 nm decreases, and the accumulation rate of Fe and total formate decreases. 15.5 g of carbon with 1.6 L of NCCC degraded solvent reduces the NH_3 production rate by 0.4 mmol/kg-hr.
- The amount of Fe removed by the carbon bed is larger than the result calculated from the solvent inventory and concentration difference of Fe in solvent. In both experiments, the Fe concentration decreased by 0.07 mmol/kg solvent, but 0.30 mmol/kg solvent and 0.12 mmol/kg solvent Fe were removed by the activated carbon in HTOR 28 and 29, respectively. This is because other soluble Fe can dissolve into the solvent to replace the dissolved Fe in the solvent that is adsorbed by the carbon.
- Combining carbon treating and nitrogen sparging is more effective in oxidation mitigation than applying the methods separately. Observations included a decrease in NH_3 production rate, OPZ, UV-Vis absorbance at 320 nm, accumulation rate of Fe, and total formate.
- The effects of carbon treating last when the carbon is bypassed, possibly due to the removal of catalytic degradation products. Therefore, it is better to apply carbon treating in the early stages of oxidation.

Carbon treating removes degradation products that can complex with Fe^{3+} to absorb at 320 nm.

Acknowledgements

This work was supported by DOE Award No. DE-FE0031861.

This report was prepared as an account of work sponsored by an agency of the United States Government. Neither the United States Government nor any agency thereof, nor any of their employees, makes any warranty, express or implied, or assumes any legal liability or responsibility for the accuracy, completeness, or usefulness of any information, apparatus, product, or process disclosed, or represents that its use would not infringe privately owned

rights. Reference herein to any specific commercial product, process, or service by trade name, trademark, manufacturer, or otherwise does not necessarily constitute or imply its endorsement, recommendation, or favoring by the United States Government or any agency thereof. The views and opinions of authors expressed herein do not necessarily state or reflect those of the United States Government or any agency thereof.

The authors have financial interests in intellectual property owned by the University of Texas that includes ideas reported in this paper.

References

[1] Freeman SA, Dugas R, Wagener DH, Nguyen T, Rochelle GT. Carbon dioxide capture with concentrated, aqueous piperazine. International Journal of Greenhouse Gas Control 2010; 4(2):119–24.

[2] Nielsen PT. Oxidation of Piperazine in Post-Combustion Carbon Capture. Ph.D. dissertation, University of Texas at Austin. 2018.

[3] Kohl, AL, Nielsen RB. **1997**. Gas Purification, fifth ed. Gulf Pub, Houston.

[4] Cousins A, Nielsen P, Huang S, Cottrell A, Chen E, Rochelle GT, Feron PH. "Pilot-scale evaluation of concentrated piperazine for CO_2 capture at an Australian coal-fired power station: Duration experiments." *Greenhouse Gases: Science and Technology* **2015**;5(4):363-73.

[5] Freeman SA. *Thermal Degradation and Oxidation of Aqueous Piperazine for Carbon Dioxide Capture*. The University of Texas at Austin. Ph.D. Dissertation. **2011**.

[6] Flø NE, Faramarzi L, Cazenove TD, Hvidsten OA, Morken AK, Hamborg ES, Vernstad K, Watson G, Pedersen S, Cents T, Fostås BF, Shah MI, Lombardo G, Gjernes E. "Results from MEA Degradation and Reclaiming Processes at the CO_2 Technology Centre Mongstad. "Energy Procedia, 2017;114:1307–1324.

[7] Moser, Peter and Wiechers, Georg and Schmidt, Sandra and Veronezi Figueiredo, Roberta and Skylogianni, Eirini and Garcia Moretz-Sohn Monteiro, Juliana, Conclusions from 3 Years of Continuous Capture Plant Operation Without Exchange of the Amp/Pz-Based Solvent at Niederaussem – Insights into Solvent Degradation Management (October 27, 2022). Proceedings of the 16th Greenhouse Gas Control Technologies Conference (GHGT-16) 23-24 Oct 2022, Available at SSRN: https://ssrn.com/abstract=4274015 or http://dx.doi.org/10.2139/ssrn.4274015

[8] Wu Y, Rochelle GT. Effects of Carbon Treating on Piperazine Oxidation in Pilot Plant Testing of

PZASTM. International Journal of Greenhouse Gas Control. 2021; 112:103502.

[9] Wu Y. Mitigation Methods for Piperazine Oxidation in Post-Combustion Carbon Capture. Ph.D. dissertation, University of Texas at Austin. 2022.

[10] Sexton AJ. Amine Oxidation in CO_2 Capture Process. The University of Texas at Austin. Ph.D. Dissertation. 2008.

[11] Rochelle GT, Wu Y, Chen E, Akinpelumi K, Fischer KB, Gao T, Liu CT, Selinger JL. "Pilot Plant Demonstration of Piperazine with the Advanced Flash Stripper." International Journal of Greenhouse Gas Control. 2021; 84: 72–81.

Appendix A. Script of Analytical Methods

Table A-1. Scripts for Anion IC

{Initial Time}	Instrument Setup	
	DC.Compartment_TC.AcquireExclusiveAccess	
	DC.Column_TC.AcquireExclusiveAccess	
	Sampler.AcquireExclusiveAccess	
	Wait	Sampler.Ready, Run=Hold, Timeout=Infinite
	DC.Suppressor1.PowerMode	Legacy
	Sampler.DiverterValve	Position_1
	Wait	Sampler.Ready, Run=Hold, Timeout=Infinite
	Pump_1.Flow	1.6 [ml/min]
	Pump_1.Pressure.UpperLimit	5000 [psi]
	Pump_1.%A.Equate	%A
	Pump_1.Pressure.LowerLimit	200 [psi]
	Sampler.CycleTime	0 [min]
	Sampler.LoopOverfill	5
	Sampler.InjectMode	PushSeqFull

	Sampler.BufferWashFactor	2
	Sampler.WashDispSpeed	20.0 [µl/s]
	Sampler.InjectWash	Both
	Sampler.WashSpeed	20.0 [µl/s]
	Sampler.WashVolume	500.0 [µl]
	Sampler.SampleHeight	2.000 [mm]
	Sampler.WasteSpeed	20.0 [µl/s]
	Sampler.DispenseDelay	2.0 [s]
	Sampler.DispSpeed	5.0 [µl/s]
	Sampler.DrawSpeed	10.0 [µl/s]
	Sampler.DrawDelay	2.0 [s]
	Sampler.DilutionMixDispenseSpeed	60.0 [µl/s]
	Sampler.DilutionMixIterations	3
	Sampler.DilutionMixSpeed	30.0 [µl/s]
	DC.Column_TC.Mode	On
	DC.Column_TC.TemperatureSet	30.00 [°C]
	DC.Compartment_TC.Mode	On
	DC.Compartment_TC.TemperatureSet	15.00 [°C]
	DC.Suppressor1.Type	ADRS_4mm
	DC.Suppressor1.Carbonate	0.0 [mM]
	DC.Suppressor1.Bicarbonate	0.0 [mM]
	DC.Suppressor1.Hydroxide	40.0 [mM]
	DC.Suppressor1.Tetraborate	0.0 [mM]
	DC.Suppressor1.OtherEluent	0.0 [mN]
	DC.Suppressor1.RecommendedCurrent	159 [mA]
	DC.Suppressor1.CurrentSet	159 [mA]
	CDet1.Rise_Time	0.50 [s]
	CDet1.Data_Collection_Rate	5.0 [Hz]
	CDet1.CellHeater.Mode	On
	CDet1.CellHeater.TemperatureSet	35.00 [°C]
	CDet1.Temperature_Compensation	1.7 [%/°C]
	Pump_1.Curve	5
	EluentGenerator.EGC_1.CR_TC	On
	Sampler.PunctureOffset	3 [mm]
-3	Equilibration	Duration = 3.000 [min]
	EluentGenerator.EGC_1.Concentration	2.00 [mM]
0	Inject	
	Wait	Sampler.CycleTimeState, Run=Hold, Timeout=Infinite
	Sampler.Inject	

0	Start Run	
	Pump_1.Pump_1_Pressure.AcqOn	
	CDet1.CD_1.AcqOn	
	CDet1.CD_1_Total.AcqOn	
	CDet1.Autozero	
0	Run	Duration = 50.000 [min]
0.1		
	Sampler.ReleaseExclusiveAccess	
	DC.Column_TC.ReleaseExclusiveAccess	
	DC.Compartment_TC.ReleaseExclusiveAccess	
17		
	EluentGenerator.EGC_1.Concentration	2.00 [mM]
27		
	EluentGenerator.EGC_1.Concentration	40.00 [mM]
40		
	EluentGenerator.EGC_1.Concentration	40.00 [mM]
45		
	EluentGenerator.EGC_1.Concentration	2.00 [mM]
50		
	EluentGenerator.EGC_1.Concentration	2.00 [mM]
50	Stop Run	
	Pump_1.Pump_1_Pressure.AcqOff	
	CDet1.CD_1.AcqOff	
	CDet1.CD_1_Total.AcqOff	
50	Post Run	Duration = 0.000 [min]
End		

Table A-2. Scripts for Cation IC

{Initial Time}	Instrument Setup	
	DC.Compartment_TC.AcquireExclusiveAccess	
	DC.Column_TC.AcquireExclusiveAccess	
	Sampler.AcquireExclusiveAccess	
	Wait	Sampler.Ready, Run=Hold, Timeout=Infinite
	DC.Suppressor1.PowerMode	Legacy
	Sampler.DiverterValve	Position_2
	Wait	Sampler.Ready, Run=Hold, Timeout=Infinite

	CationPump.Flow	1 [ml/min]
	CationPump.Pressure.UpperLimit	5000 [psi]
	CationPump.%A.Equate	%A
	CationPump.Pressure.LowerLimit	200 [psi]
	Sampler.CycleTime	0 [min]
	Sampler.LoopOverfill	5
	Sampler.InjectMode	PushSeqFull
	Sampler.BufferWashFactor	2
	Sampler.WashDispSpeed	20.0 [µl/s]
	Sampler.InjectWash	Both
	Sampler.WashSpeed	20.0 [µl/s]
	Sampler.WashVolume	500.0 [µl]
	Sampler.SampleHeight	2.000 [mm]
	Sampler.WasteSpeed	20.0 [µl/s]
	Sampler.DispenseDelay	2.0 [s]
	Sampler.DispSpeed	5.0 [µl/s]
	Sampler.DrawSpeed	10.0 [µl/s]
	Sampler.DrawDelay	2.0 [s]
	Sampler.DilutionMixDispenseSpeed	60.0 [µl/s]
	Sampler.DilutionMixIterations	3
	Sampler.DilutionMixSpeed	30.0 [µl/s]
	DC.Column_TC.Mode	On
	DC.Column_TC.TemperatureSet	30.00 [°C]
	DC.Compartment_TC.Mode	On
	DC.Compartment_TC.TemperatureSet	15.00 [°C]
	DC.Suppressor1.Type	CDRS_4mm
	DC.Suppressor1.H2SO4	0.0 [mM]
	DC.Suppressor1.MSA	11.0 [mM]
	DC.Suppressor1.RecommendedCurrent	33 [mA]
	DC.Suppressor1.OtherEluent	0.0 [mN]
	DC.Suppressor1.CurrentSet	33 [mA]
	CDet1.Rise_Time	1.00 [s]
	CDet1.Data_Collection_Rate	5.0 [Hz]
	CDet1.CellHeater.Mode	On
	CDet1.CellHeater.TemperatureSet	35.00 [°C]
	CDet1.Temperature_Compensation	1.7 [%/°C]
	CationPump.Curve	5
	EluentGenerator.EGC_1.CR_TC	On
	Sampler.PunctureOffset	3 [mm]
-3	Equilibration	Duration = 3.000 [min]
	EluentGenerator.EGC_1.Concentration	5.50 [mM]

0	Inject	
	Wait	Sampler.CycleTimeState, Run=Hold, Timeout=Infinite
	Sampler.Inject	
0	Start Run CationPump.CationPump_Pressure.AcqOn	
	CDet1.CD_1.AcqOn	
	CDet1.CD_1_Total.AcqOn	
	CDet1.Autozero	
0	Run	Duration = 50.000 [min]
0.1		
	Sampler.ReleaseExclusiveAccess	
	DC.Column_TC.ReleaseExclusiveAccess DC.Compartment_TC.ReleaseExclusiveAccess	
8.5		
	EluentGenerator.EGC_1.Concentration	5.50 [mM]
17		
	EluentGenerator.EGC_1.Concentration	11.00 [mM]
37		
	EluentGenerator.EGC_1.Concentration	11.00 [mM]
40		
	EluentGenerator.EGC_1.Concentration	5.50 [mM]
50		
	EluentGenerator.EGC_1.Concentration	5.50 [mM]
50	Stop Run CationPump.CationPump_Pressure.AcqOff	
	CDet1.CD_1.AcqOff	
	CDet1.CD_1_Total.AcqOff	
50	Post Run	Duration = 0.000 [min]
End		

395

396